Journal of Statistical Physics, Vol. 98, Nos. 1/2, 2000

Monte Carlo Study of Localization on a One-Dimensional Lattice

Hongyu Guo[1] **and Bruce N. Miller**[1]

Received May 27, 1999; final August 20, 1999

We study the equilibrium properties of a single quantum particle interacting with a classical lattice gas. We develop a path-integral formalism in which the quantum particle is represented by a closed, variable-step random walk on the lattice. After demonstrating that a Metropolis algorithm correctly predicts the properties of a free particle, we extend it to investigate the behavior of the quantum particle interacting with the lattice gas. Evidence of weak localization is observed under conditions of quenched disorder, while self-trapping clearly occurs for the fully annealed system. Compared with continuous space systems, convergence of Monte Carlo simulations in this minimum model is orders of magnitude faster in cpu time. Therefore the system behavior can be investigated for a much larger domain of thermodynamic parameters (e.g., density and temperature) in a reasonable time.

KEY WORDS: localization; self-trapping; path integral; quantum Monte Carlo; electron; positron; lattice gas.

I. INTRODUCTION

The subject matter considered in our work focuses on systems in which a single light particle interacts with more massive atoms and molecules. The light particle obeys the laws of quantum mechanics while the massive atoms can be treated classically. Examples of light particles are electrons, positrons, or positronium. This scenario is important for understanding electron transport in insulating materials, weakly ionized plasmas, and any other situation which can be modelled by an excess (or solvated) electron in a classical gas, liquid, or solid.(1) It also applies to lifetime studies of positrons produced by radioactive sources which have been injected into various materials.(2)

[1] Department of Physics, Texas Christian University, Fort Worth, Texas 76129.

0022-4715/00/0100-0347$18.00/0

Depending on the density or temperature, different qualitative behaviors of the light quantum particle (hereafter qp) become manifest. At high temperature and low density (i.e., in a dilute gas) the thermalized qp has a short wavelength compared with the mean interatomic spacing and undergoes a sequence of independent, random, scatterings from the constituent atoms or molecules.[3] As the region of the liquid-vapor critical point is approached, interesting and non-intuitive behavior occurs in low temperature systems such as helium and neon.[4] Large, nonlinear, changes are seen in the density dependence of the electron mobility[5, 6] and the positron and positronium annihilation rate[4] which qualitatively suggest that the qp has become self-trapped in a bubble or droplet of the fluid which it helps to create,[7] depending on whether the net qp-atom interaction is repulsive (bubble) or attractive (droplet). In the vicinity of the triple point, both spectroscopic and lifetime measurements suggest that the qp is propagating in the conduction band of the dense liquid.[8] Qualitative changes are also found in the critical region of fluids with higher critical temperatures, but the transition is less sharp.[3, 4] Heuristic theories which seem to be locally applicable are available for each of these scenarios,[1, 2, 7–9] but a successful analytic theory for the complete range of temperature and density is lacking. It is encouraging that recent efforts are addressing this problem.[10]

An important consideration is the time scale, τ, which is available for the measurement process. Of course, in the case of the positron or positronium, the lifetime provides a natural limit for this quantity with the vacuum ortho-positronium lifetime of 140 ns providing the upper bound.[2] However, there is also an effective lifetime for the excess electron resulting from its eventual chemical bonding to an atom or molecule, and referred to as the association time.[6] Thus, for experiments in which electron currents or positron lifetimes are measured, an important question is whether the classical host has sufficient time to respond to the presence of the qp. In general there are three possibilities: (1) the qp is non-thermal, (2) the qp thermalizes but the host does not respond (quenched host), or (3) the system completely equilibrates (annealed host). Complete self-trapping, in which the host has time to redistribute itself into a local bubble or droplet, apparently occurs in He in the critical region and requires case three. However, disorder induced (Anderson) localization[11] is still possible in case two. Although the question of thermalization has been raised in the case of positron decay in xenon,[12] at present a systematic investigation of thermalization times is lacking. In fact, it is possible that there is a threshold temperature above which localized or self-trapped states don't occur with significant probability.

Theoretical models, such as mean field theory, in which the classical atoms respond to the potential induced by a single, optimal, quantum state

have been used to describe self-trapped states. They seem to work well near the critical point of He,[7] but not for gases with critical points at higher temperatures, such as Ar and Xe,[13] where the observed nonlinear density dependence of the Ps and o-Ps decay rate varies much more gradually than the theory predicts. In contrast, independent particle models based on a spherical Wigner Seitz cell, which place the qp at the bottom of the conduction band, seem to be applicable in liquids near the triple point.[1, 6, 8, 9] However, there is no single model which succeeds everywhere, and all theories are either semi-empirical or require an uncontrolled approximation.

The Feynman–Kac path integral[14] provides the only theoretical method for exploring a model Hamiltonian directly. In this formalism, a single quantum particle is replaced by a closed harmonic chain of say p pseudo-particles with a temperature dependent force constant, each interacting with the host system through a p-reduced potential. The predictions are exact in the limit $p \to \infty$. The path integral has been used to predict the decay rate of the positron[15] and ortho-positronium[16] in xenon and to study quantum states of electrons[17] in dense gases. These computations have proven useful for elucidating behavior which could not be explained by mean field theory. For example, it was demonstrated that density fluctuations in the decay rate are of the same order as the mean in a region surrounding the liquid-vapor critical point.[18] Relying on "smart" Monte Carlo algorithms, the main difficulty encountered with PIMC (path integral Monte Carlo) is that the convergence is extremely slow. This results in a lack of confidence in some earlier results (for an excess electron) and strong limitations on the range of parameters which can be explored systematically, so that it is difficult to build up a good qualitative picture.

Chandler *et al.* have combined the path integral formalism with nonperturbative fluid structure approximations to develop an analytic theory for the equilibrium properties of an annealed qp-fluid system.[19] Using well known closures, Chen and Miller found that, in comparison with PIMC predictions, the theory seriously underestimates the deviations from free particle behavior below the critical density.[20–22] Whether other closures are more promising remains to be seen.

Then purpose of this work is to introduce a simple Hamiltonian which can be used to make numerically accurate predictions over a wide parameter range. We sacrifice some features of the real system in order to be able to explore essential features of the quantum particle behavior with confidence. Our system consists of a quantum particle on a one dimensional lattice interacting with massive atoms. The space is discrete, and both the qp and the atoms live on the lattice sites. The atoms may have a periodic distribution or may be distributed randomly. For the qp we chose a Hamiltonian which is the discrete space analogue of the usual continuous

version. In form it is similar to the tight binding Hamiltonian.[23] First we study the free particle case in which the atoms are absent. The equilibrium properties can be determined analytically by standard methods. We then develop a path integral approach for modeling the system and compare its predictions for the free particle mean energy, potential energy, and correlation function with the exact analytic expressions. This agrees perfectly with the analytical results. We then use the method to study the physical properties in the presence of atoms; first, with atoms periodically distributed on the lattice, then with quenched disorder and, finally, fully annealed. It is important to test the path integral approach for each of these cases, as the former must result in propagating qp states while the latter is subject to Anderson localization. As expected, we find that free particle behavior prevails in the high temperature limit. At finite temperature the quenched disordered system shows a gradual trend toward increasing (Anderson) localization with decreasing temperature while direct evidence of qp propagation is observed for the exactly periodic atom distribution. We find that the fully annealed system exhibits strong localization (i.e., self-trapping) as the,temperature is reduced. Finally, to get some idea of the parameter range where mean field theories can be expected to work, we compare the numerically accurate PIMC predictions with those of mean field theory.

II. DESCRIPTION OF THE MODEL

We study a one dimensional system of a light quantum particle (think of an electron, positron, etc.) interacting with more massive atoms. We suppose that the temperature is sufficiently high that the atoms can be treated classically. The lattice sites are occupied by atoms but some lattice sites are left empty. The space for the quantum particle is also discrete: i.e., the qp also lies only on the lattice sites. The qp should obey Schrodinger's equation

$$\hat{H}\,|\Psi\rangle = E\,|\Psi\rangle \tag{1}$$

where $\hat{H}$ is the Hamiltonian operator, E is the energy eigenvalue, and $|\Psi\rangle$ the state vector of the qp.

For ease of calculations it is convenient to employ second quantization. Let $|j\rangle$ denote the state in which the quantum particle is on lattice site j. Then the set $\{|j\rangle : j = ..., -L, ..., -2, -1, 0, 1, 2, ..., L, ...\}$ forms a basis for our state space. In addition, let $|\ \rangle$ denote the vacuum state. We define linear annihilation operators c_j and creation operators c_j^+ on the basis vectors as follows:

$$c_j | \ \rangle = 0 \tag{2}$$

$$c_j |k\rangle = \delta_{j,k} | \ \rangle \tag{3}$$

$$c_j^+ | \ \rangle = |j\rangle \tag{4}$$

$$c_j^+ |k\rangle = 0 \tag{5}$$

We also assert the periodic boundary condition

$$\psi_{L+1} = \psi_1 \tag{6}$$

When the space is changed from continuous to discrete, the differential operators in the Hamiltonian should be changed to difference operators accordingly. The corresponding Hamiltonian is

$$\hat{H} = 2t - t \sum_j (c_j^+ c_{j+1} + c_{j+1}^+ c_j) + \sum_j v_j c_j^+ c_j \tag{7}$$

where v_j is the potential energy of the qp on lattice site j. In our model we simply take

$$v_j = \varepsilon n_j \tag{8}$$

where n_j is the number of atoms on lattice site j, $(n_j = 0, 1)$ and with the choice

$$t = \frac{\hbar^2}{2ma^2} \tag{10}$$

in which m is the mass of the qp and a is the lattice spacing, we get the discrete approximation of the continuous Hamiltonian. This happens to be the Hamiltonian known from the tight binding model.[22] Without loss of generality we choose units such that $t = 1$ in all of the following.

III. FREE PARTICLE ON THE LATTICE

When there is an interaction between the light particle and the atoms, generally the problem cannot be solved analytically. We are going to employ a Monte Carlo calculation by way of a discrete version of the Feynman–Kac path integrals[13] to study the system. In the free particle case there are no atoms at all, $v_j = 0$ for any j, and we can get the exact analytical solution of the Schrodinger equation. We also carry out Monte Carlo calculations for the free particle case so that we can compare them

with the exact analytical solutions. For the interacting case we can only rely on our Monte Carlo calculations.

1. Analytical Solution

1.1. Energy Spectrum and Eigenstates. For the free particle case, it is easy to see we have the following solution for the eigenstates of the Schrodinger equation

$$\psi_j^{(\alpha)} = \frac{1}{\sqrt{L}} \exp\left(\frac{2\pi i \alpha j}{L}\right), \qquad \alpha = 1, 2, ..., L \tag{11}$$

where L is the lattice size. Substitute this solution into Eq. (1), notice $v_j = 0$, and we have the energy eigenvalues:

$$E^{(\alpha)} = 2t - 2t \cos\frac{2\pi\alpha}{L}, \qquad \alpha = 1, 2, ..., L \tag{12}$$

This is the energy spectrum. If $L \to \infty$, we get a single continuous energy band with two fold degeneracy because for each energy $E^{(\alpha)}$ there are two different states $\Psi^{(\alpha)}$ and $\Psi^{(L-\alpha)}$ carrying the same energy while having the opposite direction of energy flux.

1.2. Canonical Ensemble. We study the canonical ensemble of such free particle systems at finite temperature. We compute the mean energy of the qp, its mean square fluctuation, and the quantum correlation of the qp with itself along the lattice.

The equilibrium density matrix of such an ensemble is $\exp(-\beta\hat{H})$ where, as usual, β is the inverse temperature in appropriate units. We need to calculate the partition function per lattice site, Z/L,

$$\frac{Z}{L} = \frac{1}{L} \sum_{\alpha=1}^{L} \exp(-\beta E^{(\alpha)}) \tag{13}$$

This can be expressed as

$$\frac{Z}{L} = e^{-2\beta t} I_0(2\beta t) \tag{14}$$

in the limit of $L \to \infty$, where I_0 is the 0th order modified Bessel function.

The expectation value of the energy is

$$\langle \hat{H} \rangle = 2t + \langle \hat{H}' \rangle \tag{15}$$

where H' is the typical tight binding hamiltonian and here the angle brackets represent the thermal average:

$$\hat{H}' = \hat{H} - 2t$$

$$= -t \sum_j (c_j^+ c_{j+1} + c_{j+1}^+ c_j) \tag{16}$$

$$\langle \hat{H}' \rangle = \left(\frac{1}{L} \langle \hat{H}' e^{-\beta \hat{H}} \rangle \right) \Big/ \left(\frac{Z}{L} \right) \tag{17}$$

With a little calculation, we find

$$\langle \hat{H}' \rangle = -2tI_1(2\beta t)/I_0(2\beta t) \tag{18}$$

Similarly, we also obtain the energy fluctuation per site, as

$$\langle \hat{H}^2 \rangle - \langle \hat{H} \rangle^2 = 2t^2 + 2t^2 \frac{I_2(2\beta t)}{I_0(2\beta t)} - 4t^2 \frac{I_1^2(2\beta t)}{I_0^2(2\beta t)} \tag{19}$$

where, in the above and in the remainder of the paper, I_n is the modified Bessel function of order n.

Now we investigate the correlation function. We define

$$G_1(n) = \left\langle \sum_j \psi_j^* \psi_{j+n} \right\rangle \tag{20}$$

as the qp–qp correlation function. Since ψ_{j+n} is the wave function ψ_j displaced by n lattice sites, $G_1(n)$ provides a measure of the mean spread of the qp along the lattice. We will investigate other correlations, such as the atom–qp correlation function, later.

Now, from (11),

$$G_1(n) = \frac{\sum_\alpha (1/L) \exp(-\beta E^{(\alpha)}) \exp(2n\pi\alpha i/L)}{\sum_\alpha (1/L) \exp(-\beta E^{(\alpha)})} \tag{21}$$

Skipping a lengthy calculation, finally we find

$$G_1(n) = \frac{I_n(2\beta t)}{I_0(2\beta t)} \tag{22}$$

in the limit of $L \to \infty$.

2. Path Integral Analogue

In general, for an arbitrary interacting system, there is no direct way to compute the quantum trace. Lacking a quantum computer, we have to find some equivalent classical system which we can sample by standard means. For each physical observable we want to investigate, we need to construct a corresponding "classical" operator in the path integral formalism. These transformed operators become the random functions which are averaged in the Monte Carlo calculation.

2.1. Partition Function. To demonstrate the path integral re-formulation, we start with the partition function. In the $|j\rangle$ representation the partition function is

$$Z = \mathrm{Tr}\, e^{-\beta\hat{H}} = \sum_{j_1} \langle j_1|\, e^{-\beta\hat{H}}\, |j_1\rangle \tag{23}$$

We split the operator into p factors,

$$e^{-\beta\hat{H}} = [e^{-\beta\hat{H}/p}]^p = e^{-\beta\hat{H}/p} e^{-\beta\hat{H}/p} \cdots e^{-\beta\hat{H}/p} \tag{24}$$

and insert the identity operators,

$$\sum_{j_\alpha} |j_\alpha\rangle\langle j_\alpha| = 1 \tag{25}$$

Making use of the Trotter formula,[13] we have

$$\begin{aligned} Z &= \sum_{j_1}\sum_{j_2}\cdots\sum_{j_p} \langle j_1|\, e^{-\beta\hat{H}/p}\, |j_2\rangle\langle j_2|\, e^{-\beta\hat{H}/p}\, |j_3\rangle \cdots \langle j_p|\, e^{-\beta\hat{H}/p}\, |j_1\rangle \\ &= \sum_{j_1}\sum_{j_2}\cdots\sum_{j_p} \prod_{\alpha=1}^{p} \langle j_\alpha|\, e^{-\beta\hat{H}/p}\, |j_{\alpha+1}\rangle \end{aligned} \tag{26}$$

where

$$j_{p+1} = j_1 \tag{27}$$

We calculate the matrix element in Eq. (26) to be

$$\langle j|\, e^{-\beta\hat{H}/p}\, |k\rangle = I_{j-k}(2\beta t/p) \tag{28}$$

so finally we obtain the partition function as

$$Z = \sum_{j_1}\sum_{j_2}\cdots\sum_{j_p} \prod_{\alpha=1}^{p} I_{j_\alpha - j_{\alpha+1}}(2\beta t/p) \tag{29}$$

where the summation is over all $j_1, j_2, ..., j_p$. We can identity the sequence $\mathbf{j} = (j_1, j_2, ..., j_p)$ with a p step closed random walk on the lattice which starts at j_1 and has steps with displacement

$$s_\alpha = j_{\alpha+1} - j_\alpha \tag{30}$$

and the factor

$$\prod_{\alpha=1}^{p} I_{j_\alpha - j_{\alpha+1}}(2\beta t/p) \tag{31}$$

as the probability (when properly normalized) assigned to each random walk.

Notice that a sample walk $j_1, j_2, ..., j_p$ is required to satisfy the constraint $j_{p+1} = j_1$ or

$$\sum_{\alpha=1}^{p} s_\alpha = 0 \tag{32}$$

so the random walk is closed.

We can also interpret the form of Z from another point of view. We define

$$\Phi(\mathbf{j}) = \Phi(j_1, j_2, ..., j_p) = -\frac{1}{\beta} \sum_{\alpha=1}^{p} \ln I_{j_\alpha - j_{\alpha+1}}(2\beta t/p) \tag{33}$$

and

$$\varphi(j) = -\frac{1}{\beta} \ln I_j(2\beta t/p) \tag{34}$$

Then

$$\Phi(j_1, ..., j_p) = \sum_{\alpha=1}^{p} \varphi(j_\alpha - j_{\alpha+1}) \tag{35}$$

and

$$\prod_{\alpha=1}^{p} I_{j_\alpha - j_{\alpha+1}}(2\beta t/p) = \exp[-\beta\Phi(j_1, j_2, ..., j_p)] \tag{36}$$

We can then interpret the probability

$$\prod_{\alpha=1}^{p} I_{j_\alpha - j_{\alpha+1}}(2\beta t/p) \tag{37}$$

as the ensemble probability of certain classical systems

$$\exp[-\beta\Phi(j_1, j_2, ..., j_p)] \tag{38}$$

This classical system takes the form of a closed ring polymer on the lattice consisting of p particles with the interaction energy $\Phi(j_1, j_2, ..., j_p)$. Effectively, each polymer element is only directly coupled to it's nearest neighbors in the chain (not necessarily the nearest lattice site) through the interaction φ which depends both on β and the number of lattice sites separating each pair of polymer elements.

Our approach will be to construct random walks by generating sequences of positive and negative integers $s_1, s_2, ..., s_p$ according to the probability $P(s_1, s_2, ..., s_p)$. We will develop appropriate functions which, when averaged over a large set of walks, converge to the thermal mean of specific physical and statistical quantities, e.g., the energy and the correlation function $G_1(n)$.

2.2. Energy. We also need to find a way to calculate the average energy by the Monte Carlo method. We treat the energy in a similar manner as the partition function. As usual,

$$\hat{H} = \hat{T} + \hat{V} \tag{39}$$

where $\hat{T}$ is kinetic energy operator and $\hat{V}$ is potential energy operator. In the free particle case,

$$\hat{H} = \hat{T} = 2t - t\sum_j (c_j^+ c_{j+1} + c_{j+1}^+ c_j) \tag{40}$$

$$\hat{V} = 0 \tag{41}$$

$$\hat{T}' = \hat{H}' = -t\sum_j (c_j^+ c_{j+1} + c_{j+1}^+ c_j) \tag{42}$$

The matrix element in the $|j\rangle$ representation is easily seen to be

$$\langle j_1 | \hat{T}' | k \rangle = -t(\delta_{j_1, k-1} + \delta_{j_1, k+1}) \tag{43}$$

Then, taking the canonical average of $\hat{T}$,

$$\langle \hat{T}' \rangle = \mathrm{Tr}[\hat{T}' e^{-\beta\hat{H}}]/Z \tag{44}$$

we find

$$\mathrm{Tr}[\hat{T}' e^{-\beta\hat{H}}]$$

$$= \sum_{j_1} \sum_{j_2} \cdots \sum_{j_p} \left\{ -\frac{2t}{p} \sum_{\alpha=1}^{p} \frac{I_{j_\alpha - j_{\alpha+1}+1}(2\beta t/p)}{I_{j_\alpha - j_{\alpha+1}}(2\beta t/p)} \right\} \prod_{\alpha=1}^{p} I_{j_\alpha - j_{\alpha+1}}(2\beta t/p) \tag{45}$$

We see from Eq. (45) that the average of a physical observable $\hat{\Theta}$ has the form

$$\sum_{\text{walks}} \Theta_{\text{cl}}(\text{walk} \times \text{Probability(walk)}) \tag{46}$$

where Θ_{cl} is a function defined on a walk and is the counterpart of the quantum operator $\hat{\Theta}$ in the classical system isomorphism. Each quantum operator has a corresponding classical operator in the isomorphic ensemble of polymer systems. Thus the quantum kinetic energy operator is

$$\hat{T} = 2t - t \sum_{j} (c_j^+ c_{j+1} + c_{j+1}^+ c_j) \tag{47}$$

and its classical analogue is

$$\tau = 2t - \frac{2t}{p} \sum_{\alpha=1}^{p} \frac{I_{j_\alpha - j_{\alpha+1}+1}(2\beta t/p)}{I_{j_\alpha - j_{\alpha+1}}(2\beta t/p)} \tag{48}$$

2.3. Energy Fluctuation. We will treat the square of the energy similarly in order to compute the energy fluctuation. First we calculate the matrix element

$$\langle j_1 | \hat{T}'^2 | k \rangle = t^2(\delta_{j_1, k-2} + 2\delta_{j_1, k} + \delta_{j_1, k+2}) \tag{49}$$

The calculation is similar to that of the energy and we obtain

$$\mathrm{Tr}[\hat{T}^2 e^{-\beta\hat{H}}]$$

$$= e^{-2\beta t} \sum_{j_1} \sum_{j_2} \cdots \sum_{j_p} \left\{ 2t^2 + \frac{2t^2}{p} \sum_{\alpha=1}^{p} \frac{I_{j_\alpha - j_{\alpha+1}+2}(2\beta t/p)}{I_{j_\alpha - j_{\alpha+1}}(2\beta t/p)} \right\} \prod_{\alpha=1}^{p} I_{j_\alpha - j_{\alpha+1}}(2\beta t/p) \tag{50}$$

The classical isomorphism of $\hat{T}^2$ is therefore

$$\tau_2 = 2t^2 + \frac{2t^2}{p} \sum_{\alpha=1}^{p} \frac{I_{j_\alpha - j_{\alpha+1}+2}(2\beta t/p)}{I_{j_\alpha - j_{\alpha+1}}(2\beta t/p)} \tag{51}$$

2.4. Correlation Function. We are going to compute the correlation function using the path integral formalism. From the definition (20),

$$G_1(n) = \sum_j \psi_j^* \psi_{j+n}$$

In the occupation number representation, it takes the form

$$\hat{G}_1(n) = \sum_j c_j^+ c_{j+n} \tag{52}$$

The matrix element we need is

$$\langle j_1 | \hat{G}_1 | k \rangle = \delta_{j_1, k-n} \tag{53}$$

and the trace will be

$$\mathrm{Tr}[\hat{G}_1 e^{-\beta \hat{H}}] = \sum_{j_1} \sum_{j_2} \cdots \sum_{j_p} \left\{ \frac{1}{p} \sum_{\alpha=1}^{p} \frac{I_{j_\alpha - j_{\alpha+1}+n}(2\beta t/p)}{I_{j_\alpha - j_{\alpha+1}}(2\beta t/p)} \right\} \prod_{\alpha=1}^{p} I_{j_\alpha - j_{\alpha+1}}(2\beta t/p) \tag{54}$$

It follows that the classical analogue of qp–qp correlation function operator is

$$\Gamma_1 = \frac{1}{p} \sum_{\alpha=1}^{p} \frac{I_{j_\alpha - j_{\alpha+1}+n}(2\beta t/p)}{I_{j_\alpha - j_{\alpha+1}}(2\beta t/p)} \tag{55}$$

2.5. Generation of the Random Walks. Here we develop a Levy method for sampling the walks. Suppose $P(\mathbf{s})$ is the probability of sequence $(s_1, s_2, ..., s_p)$. Then

$$P(s_1, s_2, ..., s_p) = C \prod_{\alpha=1}^{p} I_{s_j}(2\beta t/p)\, \Delta\left(\sum_\alpha s_\alpha \right) \tag{56}$$

where

$$\Delta(x) = \begin{cases} 1 & x = 0 \\ 0 & x \neq 0 \end{cases} \tag{57}$$

and C is a normalization factor. The presence of the function Δ arises from the constraint (32) which requires the random walk to be closed. Using the Fourier representation of $\Delta(x)$

$$\Delta(x) = \frac{1}{2\pi} \int_{-\pi}^{\pi} e^{ikx}\, dx \tag{58}$$

and the identity[8]

$$\sum_{s=-\infty}^{\infty} I_s(x)\cos ks \equiv e^{x\cos k} \tag{59}$$

we find

$$C = 1/I_0(2\beta t) \tag{60}$$

We'd like to generate the sequence of numbers $j_1, j_2,..., j_p$ one after another instead of getting them at once as a group. We ask, given the first v integers in the sequence $s_1, s_2,..., s_v$, what is the conditional probability, $P(s_{v+1} \mid s_1, s_2,..., s_v)$, of getting s_{v+1} next?

As usual, the conditional probability can be expressed as

$$P(s_{v+1} \mid s_1, s_2,..., s_v) = P(s_1, s_2,..., s_{v+1})/P(s_1, s_2,..., s_v) \tag{61}$$

where

$$P(s_1, s_2,..., s_v) = C \sum_{s_{v+1}} \sum_{s_{v+2}} \cdots \sum_{s_p} \left[\prod_{\alpha=1}^{v} I_{s_\alpha}(2\beta t/p) \right] \times \left[\prod_{\alpha=v+1}^{p} I_{s_\alpha}(2\beta t/p) \right] \Delta \left(\sum_{\alpha=1}^{v} s_\alpha + \sum_{\alpha=v+1}^{p} s_\alpha \right)$$

is the joint probability for $s_1, s_2,..., s_v$ and again Δ insures the closure of each random walk.

Let

$$t_v = \sum_{\alpha=1}^{v} s_\alpha \tag{62}$$

be the displacement after v steps. Then as we did earlier by employing the Fourier representation of Δ, we have

$$\begin{aligned} &\sum_{s_{v+1}} \cdots \sum_{s_p} \left[\prod_{\alpha=v+1}^{p} I_{s_\alpha}(2\beta t/p) \right] \Delta \left(t_v + \sum_{\alpha=v+1}^{p} s_\alpha \right) \\ &\quad = \frac{1}{2\pi} \int_{-\pi}^{\pi} e^{ikt_v} \exp\left(\frac{p-v}{p} 2\beta t \cos k \right) dk \\ &\quad = I_{t_v}\left(\frac{p-v}{p} 2\beta t \right) \end{aligned} \tag{63}$$

Finally we obtain for the conditional probability,

$$P(s_{v+1} \mid s_1,..., s_v) = \frac{I_{t_{v+1}}(((p-v)/p)\, 2\beta t)\, I_{s_{v+1}}(2\beta t/p)}{I_{t_v}(((p-v)/p)\, 2\beta t)} \tag{64}$$

3. Results from the Monte Carlo Calculation

We generated random walks step by step by partitioning the unit interval by the sequence of sub-intervals $P(0 \mid s_1,..., s_v)$, $P(1 \mid s_1,..., s_v)$, $P(-1 \mid s_1,..., s_v)$, $P(2 \mid s_1,..., s_v)$, $P(-2 \mid s_1,..., s_v)$,.... We select a random number from the uniform distribution and determine which interval of the partition it occupies. Then the displacement of the random walk in this step is determined. We add up the contributions for the classical analogue of the operator for the complete random walk and finally we take the mean over all walks to get the average.

Using the computer, we calculated the energy and correlation functions over a variety of temperatures and they turned out to agree very well with the analytical results. Figure 1 shows the energy over a range of

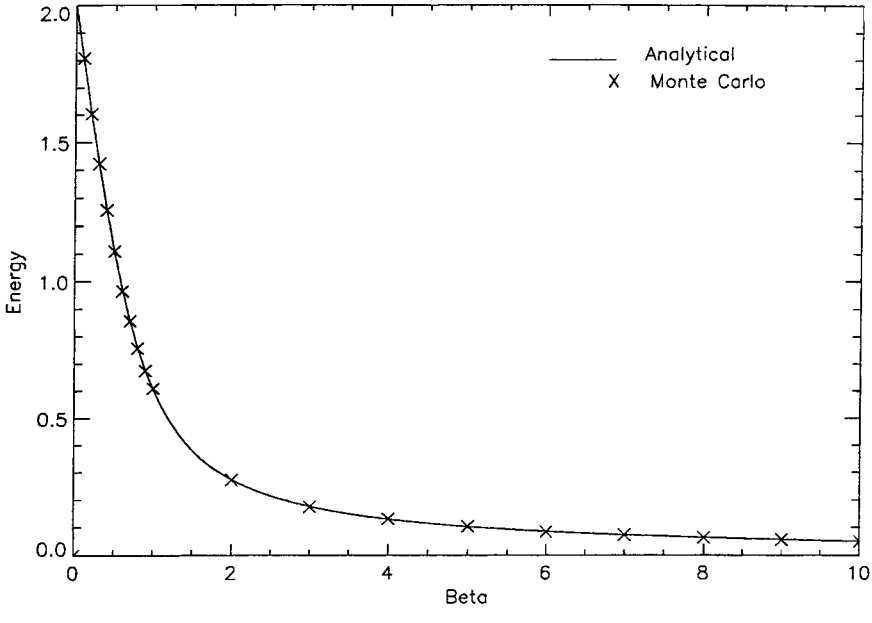

Fig. 1. Energy vs. Inverse temperature, β, for a free particle moving on the lattice. The continuous curve is a plot of the exact theoretical results. The crosses are the results of Monte Carlo simulations. The agreement is outstanding. Error bars are too small to be seen on this scale.

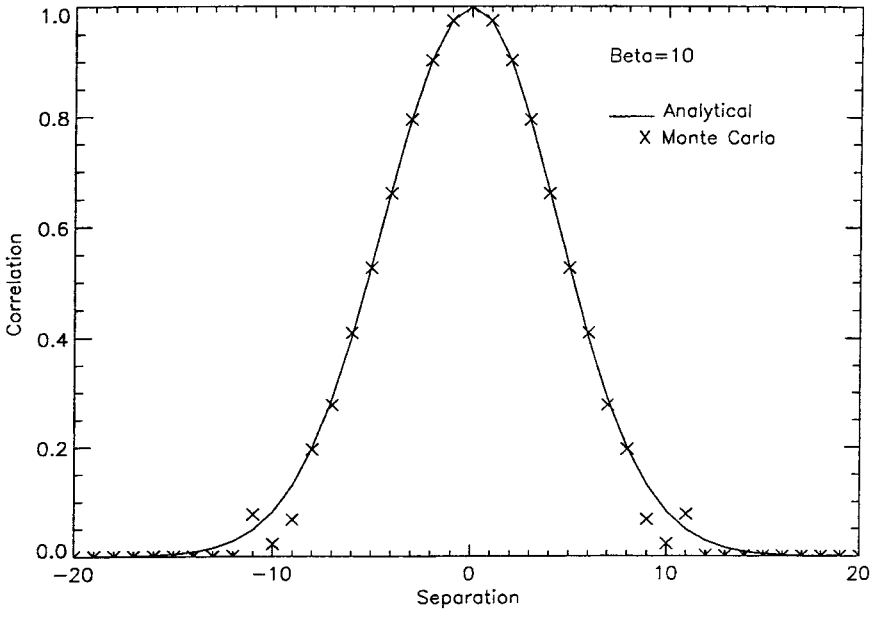

Fig. 2. Self-correlation function, $G_1(n)$, of the free quantum particle on the lattice for $\beta = 10$. As above, the curve is a plot of the exact theoretical results while the crosses represent the Monte Carlo simulations. Note the excellent agreement except near the shoulders, where the number of significant events becomes small.

temperatures. The solid line is the analytical result; and the crossed points are Monte Carlo results. In Fig. 2 we plot the qp–qp correlations vs separation n for $\beta = 10$. Again, the agreement of the Monte Carlo simulations with the analytic results is excellent. Calculations over a wide range of temperature (not shown) confirm our intuition that when the temperature is lowered the correlation just spreads out. It's important to note that, for a free particle, the discrete path integral is exact for finite Trotter number p. In practice, choosing values between 10 and 100, we obtained excellent convergence (see Fig. 1) by sampling 10^5 independent walks. Typical differences from the exact result were in the fourth decimal place for the energy.

IV. PRESENCE OF ATOMS ON THE LATTICE

1. Fixed Configurations of Atoms

Now we deal with the presence of the interaction between the qp and the atoms. This is easiest when the atoms are rigidly fixed on the lattice;

then the qp just sees the atoms as the source of an external potential field. This corresponds to the case where the influence of the lattice on the qp is one way. There is no feedback, and the lattice atoms are not aware of the presence of the qp. As before, we express the quantum operators in the path integral form. This is very similar to the case of the free particle except that the potential v_j is included as the external field.

We will consider two very different qp environments, one in which the atoms are distributed periodically on the lattice, and the other representing complete quenched disorder. These are both important. The former provides a test of the path integral formalism for dealing with propagating qp states, while the latter should induce localization via the Anderson mechanism. In each case the lattice is half filled on the average, and we choose $\varepsilon = 10.0$, i.e., a strong interaction strength, for the qp–atom interaction strength.

1.1. Metropolis Sampling. The probability of a specific walk on the lattice is now proportional to

$$\exp(-\beta V/p)\left[\prod_{\alpha=1}^{p} I_{s_\alpha}(2\beta t/p)\right] \Delta\left(\sum_{\alpha=1}^{p} s_\alpha\right)$$

Thus all averages must now include the Gibb's factor $\exp(-\beta V/p)$ as well as the product of modified Bessel functions. In contrast with the free particle, in the general interacting system the presence of this factor in the distribution function prevents us from directly sampling the probability distribution for a random walk. To deal with this complication we employ Metropolis sampling.[23] That is we still use the free particle conditional probability, expressed in Eq. (71), to generate a walk, but we then employ rejection to produce a sequence of walks which satisfies the correct distribution. Let q represent the acceptance factor,

$$q = \frac{\prod_{\alpha=1}^{p} e^{-\beta V'_{j_\alpha}}}{\prod_{\alpha=1}^{p} e^{-\beta V_{j_\alpha}}} = \frac{\exp(-(\beta/p)\sum_{\alpha=1}^{p} V'_{j_\alpha})}{\exp(-(\beta/p)\sum_{\alpha=1}^{p} V_{j_\alpha})} \tag{65}$$

where V' is the potential energy for the new walk, and V that of the previous walk. Then according to the Metropolis criteria, if $q > 1$ we automatically accept the new walk, while if $q < 1$ we only accept it with probability q. This is determined by drawing a random number on the unit interval. If it is less than q, we accept the walk. If it is greater than q, we reject it and we repeat the data for the previous walk.

For the interacting system we applied the Metropolis method to completed walks. We increased both the Trotter number, p, and the number of

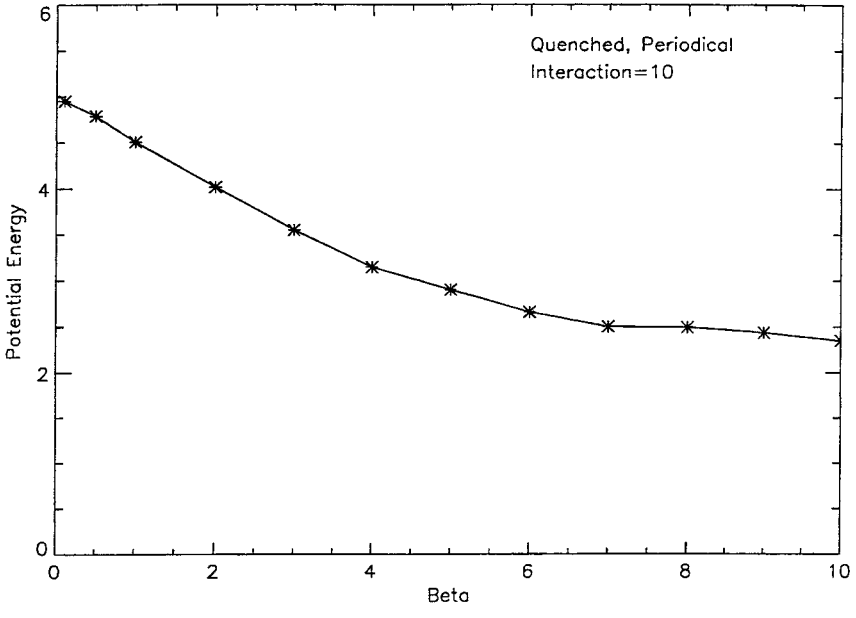

Fig. 3. Potential energy of the qp vs. β for an exactly periodic lattice in which atoms occupy alternate sites. In our dimensionless units, the qp–atom interaction strength, $\varepsilon = 10$.

independent samples until changes in mean values ceased to occur. We found excellent convergence with $p > 50$ and a total of 10^5 walks. To confine the system we applied periodic boundary conditions to both the walks and the lattice atoms with a total of L sites. The extension of the polymer was seldom greater than 10 lattice sites. By choosing L to be 300 sites in length, we avoided any noticeable finite size effects.

1.2. Form of the Operators. The expression for both kinetic energy operator and the qp–qp correlation function G_1 in the classical isomorphism remains the same in the interacting system as that for the free particle, while that for the potential energy is simply given by $V(\mathbf{n}) = \sum_{\alpha=1}^{p} \varepsilon n_{j_\alpha}$. However, in the presence of atoms, we can also define and study the atom-quantum-particle correlation function,

$$G_2(n) = \left\langle \sum_j n_j \, |\psi_{j+n}|^2 \right\rangle \tag{66}$$

In occupation number representation

$$\hat{G}_2(n) = \sum_j n_j c_{j+n}^{+} c_{j+n} \tag{67}$$

Note that we do not include $e^{-\beta V}$ in the definition of the operator.

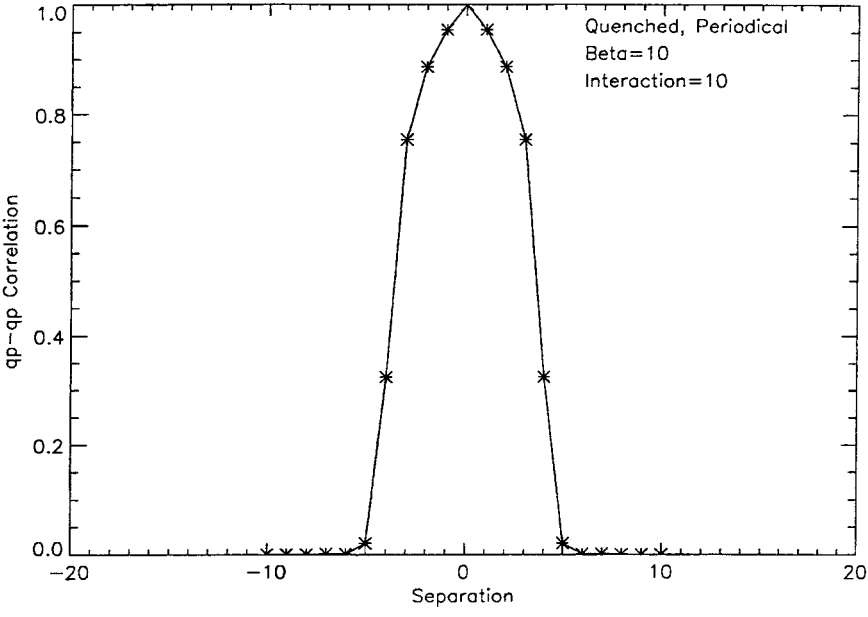

Fig. 4. Self-correlation function, $G_1(n)$, of the qp interacting with the periodic lattice for $\beta = \varepsilon = 10$. Compare this with Fig. 2 and note the shorter range and steep shoulders.

This carries information concerning the range of lattice sites over which the qp wave functions are influenced by an atom, and vice-versa. It is apparent that, on an infinite lattice, $G_2(n)$ vanishes for large n unless the distribution of atoms exhibits long range order. The calculation $G_2(n)$ is parallel to the above: We find the path integral form of this correlation function is

$$G_2(n) = (1/Z) \sum_{j_1} \sum_{j_2} \cdots \sum_{j_p} \left\{ \frac{1}{p} \sum_{\alpha=1}^{p} n_{j_\alpha - n} \right\} \times \prod_{\alpha=1}^{p} e^{-\beta V_{j_\alpha}/p} I_{j_\alpha - j_{\alpha+1}}(2\beta t/p)\, \Delta \left(\sum_{\alpha=1}^{p} s_\alpha \right) \tag{68}$$

Thus $\Gamma_2(n)$, the classically isomorphic operator to $G_2(n)$, is simply

$$\Gamma_2(n) = \frac{1}{p} \sum_{\alpha=1}^{p} n_{j_\alpha - n} \tag{69}$$

1.3. Monte Carlo Calculation for Periodic Atoms. The atoms were distributed on alternate lattice sites. We calculated the kinetic and potential energy as a function of temperature or β. We computed the qp–qp correlation functions, and also obtained the atom-qp correlations. The dependence of the kinetic energy on β is nearly the same as in the free particle case (see Fig. 1). We can see that at high temperature (small β), the behavior is nearly the same as the free particle case. That is to say, the potential energy is around 5.0. Since the interaction parameter is set to be 10.0, it means that at high temperature the qp just moves freely on the lattice and it meets an atom with a chance of one half. As shown in Fig. 3, the potential energy gradually drops with increasing β, indicating the development of correlation between the qp and lattice atoms, and the preference of the qp to sit on unoccupied sites. As shown in Fig. 4, this behavior is mirrored by the qp–qp correlation function, $G_1(n)$, which drops much more steeply than that for the free particle (compare with Fig. 2, both computed with $\beta = 10$). Figure 5 illustrates the atom-qp correlation, also at $\beta = 10$. We observe the undulating pattern arising from the periodic layout of the atoms demonstrating the long (nearly infinite) range of correlation between the qp and the lattice atoms.

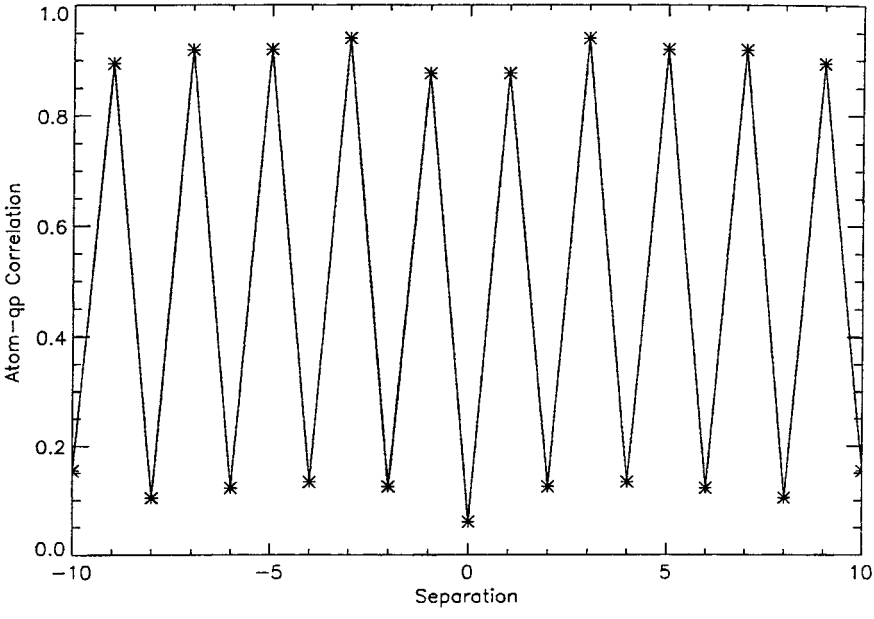

Fig. 5. The qp–atom correlation function, $G_2(n)$, for the periodic lattice with $\beta = \varepsilon = 10$. Note the evidence of propagating modes from the long range order.

2. Grand Ensemble of Disordered Quenched Lattices

Here we consider a grand canonical ensemble of random systems with varying numbers of atoms and a single qp. The number of atoms is not fixed. As above, we consider the case where the lattice is half filled on the average.

In the quenched case, we distribute the atoms independently of the qp. First we lay down the configuration of atoms by simply occupying each lattice site with an atom at random with probability 0.5. Then, for each configuration of atoms $\mathbf{n}=(n_1, n_2,..., n_L)$, where $n_j=0, 1$ is the occupation number of site j, we treat $\mathbf{n}$ as fixed when considering the qp, i.e., we allow the qp to thermalize in the field induced by the fixed atoms. Then the average of a quantum operator $\hat{\Theta}$ over walks $\mathbf{j}=(j_1,..., j_p)$ depends on $\mathbf{n}$, and we denote it by $\langle \hat{\Theta}_n \rangle$,

$$\langle \hat{\Theta}_n \rangle = \frac{\sum_{j_1,..., j_p} e^{-\beta V_{j_\alpha}/p} \Theta_{\mathrm{cl}}(\mathbf{n}, \mathbf{j}) \prod_{\alpha=1}^{p} I_{j_\alpha - j_{\alpha+1}}(2\beta t/p)}{\sum_{j_1,..., j_p} e^{-\beta V_{j_\alpha}/p} \prod_{\alpha=1}^{p} I_{j_\alpha - j_{\alpha+1}}(2\beta t/p)} \tag{70}$$

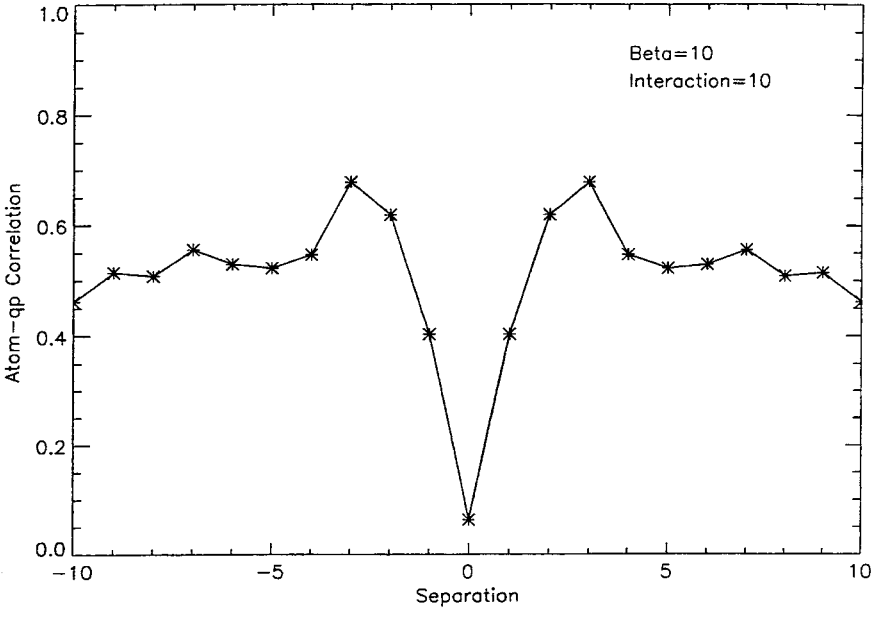

Fig. 6. The qp–atom correlation function, $G_2(n)$, for the quenched, disordered, lattice with $\beta=\varepsilon=10$. Note the lack of long range order and the evidence of a small quantum well, suggesting that weak localization occurs in the neighborhood of density fluctuations.

where Θ_{cl}, is the classical counterpart of the quantum operator $\hat{\Theta}$. By averaging over **n** we obtain the final ensemble average of $\hat{\Theta}$ as

$$\langle \hat{\Theta} \rangle = \sum_{n_1,\ldots,n_L} \frac{\prod_{\alpha=1}^{L} e^{\beta\mu n_\alpha}}{(1+\exp(\beta\mu))^L} \langle \hat{\Theta}_n \rangle \tag{71}$$

With regard to the kinetic and potential energy, as well as the qp–qp correlation function, the results of the Monte Carlo calculation for the quenched ensemble are similar to those of the periodic lattice with the same mean density. In Fig. 6 we plot the atom-qp correlations. This shows strongly the effect of Anderson localization, for around zero separation the correlation drops almost to zero, indicating that it is extremely unlikely to find the qp at an occupied lattice site, but at large displacements approaches 0.5 as it must.

3. Annealed Lattices

When the lattice is annealed, the qp can also influence the local distribution of atoms on the lattice and the influence works both ways. We

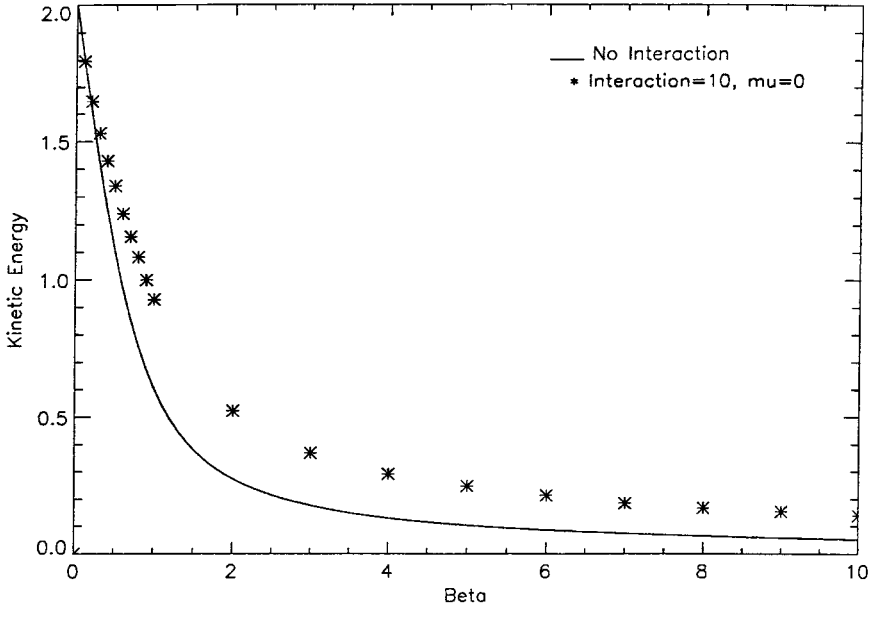

Fig. 7. Kinetic energy vs. β for the fully annealed qp–atom system. For comparison we also present the free particle calculation (smooth curve). Note that for sufficiently low temperature ($\beta > 0.5$) the kinetic energy of the qp is greater than that of the free particle. This suggests that the qp is frequently trapped in a quantum well which it helps to create.

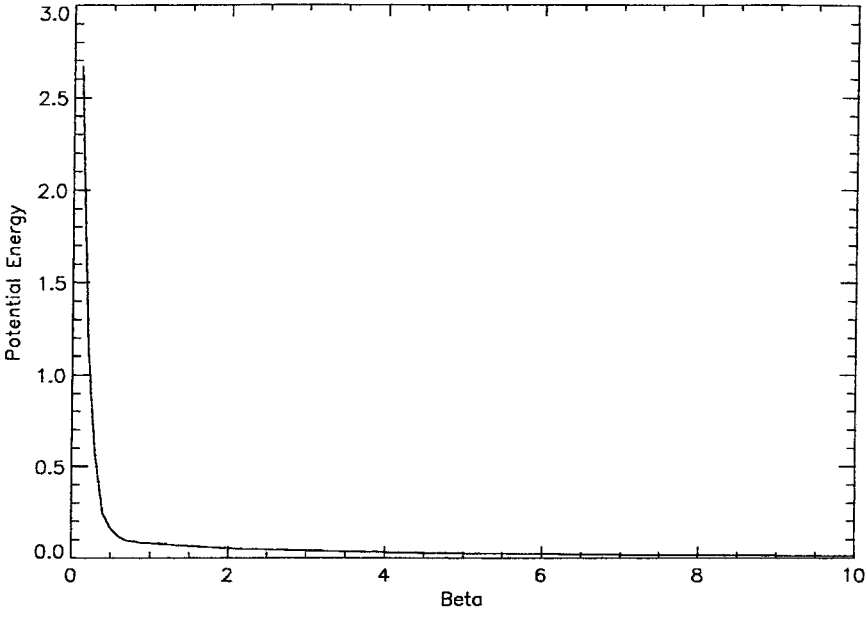

Fig. 8. Potential energy vs β for the fully annealed system. Consistent with Fig. 7 in the vicinity of $\beta \approx 0.5$ the potential energy drops rapidly from 5.0, the infinite temperature value, to nearly zero, suggesting that the qp is now trapped in a nearly atom free domain.

thus consider the qp and the atoms together as one system. The atoms are no longer simply a source for the external potential experienced by the qp. The complete density matrix is now

$$\exp\left(\beta\mu \sum_j n_j\right) \mathrm{Tr} \exp(-\beta\hat{H})$$

and the grand partition function is

$$\Xi = \sum_{\{n_j\}} e^{\beta\mu \sum_j n_j} \mathrm{Tr}\, e^{-\beta\hat{H}} \tag{72}$$

where, as usual, μ is the chemical potential.

When expressed in path integral form, (72) takes the form

$$\Xi = \sum_{n_1, n_2, \ldots, n_L} e^{\beta\mu N} \sum_{j_1, j_2, \ldots, j_p} \prod_{\alpha=1}^{p} e^{-\beta V_{j_\alpha}} I_{j_{\alpha+1}-j_\alpha}(2\beta t/p)\, \Delta\left(\sum_{\alpha=1}^{p} s_\alpha\right) \tag{73}$$

To determine the grand partition function (and all other functions) by Monte Carlo sampling, we sample the atoms $n_1, n_2, ..., n_L$ simultaneously with the random walk for the qp, $j_1, j_2, ..., j_p$.

As above, we denote $\mathbf{n} = (n_1, n_2, ..., n_L)$. Thus the pair of lattice vectors $\mathbf{n}, \mathbf{j}$ represent a microstate of the (classical) system. To proceed, we need to be able to sample the joint probability $P(\mathbf{n}, \mathbf{j})$. In the previous quenched case we sampled the conditional probability $P(\mathbf{j} \mid \mathbf{n})$, that is the probability of obtaining the random walk $\mathbf{j}$ after the atoms are previously laid down. To sample the joint probability $P(\mathbf{n}, \mathbf{j})$ we also use the standard form of the Metropolis method. As in the quenched disordered system considered earlier, we lay down the lattice atoms independently on each site with probability 0.5, and use the free particle distribution to generate the walk $\mathbf{j}$. We then construct the acceptance ratio q as above and accept or reject the $\mathbf{n}, \mathbf{j}$ pair in the usual manner.

Figures 7 through 10 illustrate the results of Monte Carlo calculations. Figure 7 shows the kinetic energy vs β, or inverse temperature. The solid line is the comparison with the free particle kinetic energy. The starred points are Monte Carlo calculations with the interaction parameter set equal to 10. We observe that the kinetic energy is higher when there is

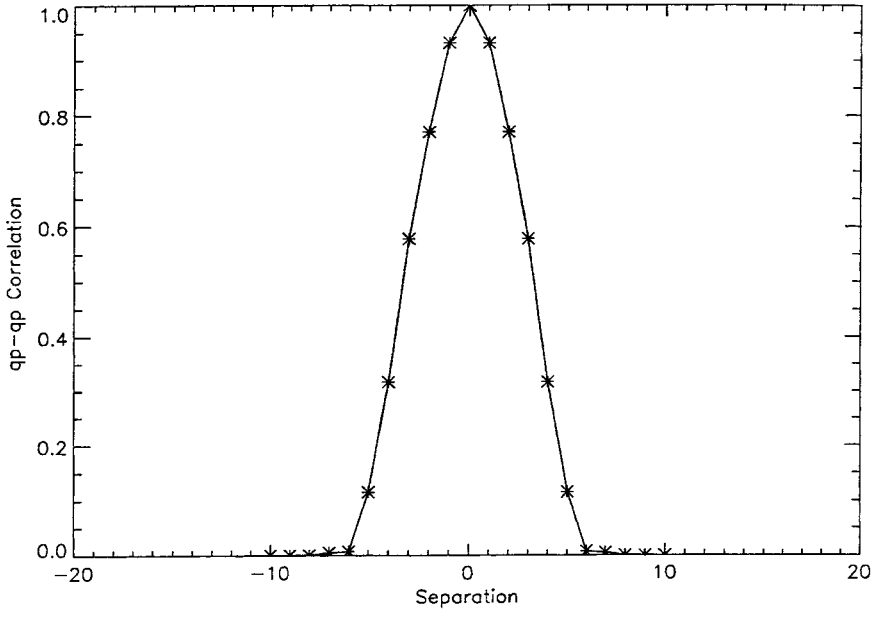

Fig. 9. Self-correlation function, $G_1(n)$, of the qp interacting with the fully annealed lattice for $\beta = \varepsilon = 10$. Compare this with Figs. 2 and 4. Note the finite range, suggesting an average well width of about 10 lattice sites.

strong interaction between the qp and the atoms. Figure 8 shows the potential energy vs β. We observe that as the temperature drops, the potential energy decreases much more rapidly than in the quenched system, dropping nearly to zero at finite temperature. Figure 9 shows that the qp–qp correlation function is narrowed compared with the free particle case. Figure 10 shows the atom-qp correlation. We see that it goes to zero sharply at zero separation. Figures 7, 8 and 10 strongly indicate the effect of self trapping. When the lattice is annealed, the qp is able to influence its environment by enlarging the potential well created by a group of adjacent lattice sites which is free of atoms when the temperature is low and the interaction is strong. Consequences are an enhanced kinetic energy (from the uncertainty principle), a reduced potential energy (since the qp is primarily occupying empty sites) and a region of strong qp–atom positional anti-correlation. Similar behavior has been observed experimentally with positrons thermalized in helium near the critical point.[2, 4]

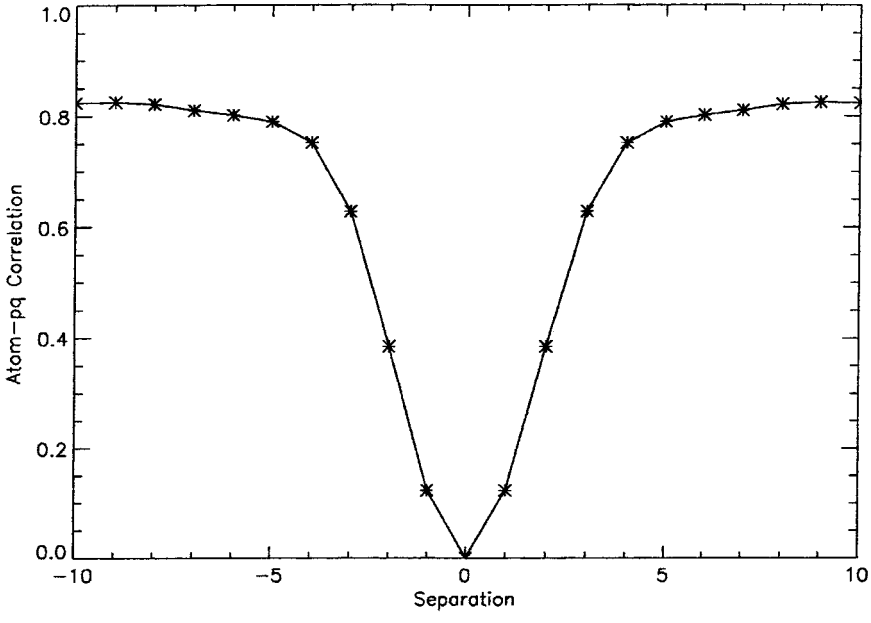

Fig. 10. The qp–atom correlation function, $G_2(n)$, for the fully annealed system with $\beta = \varepsilon = 10$. Note the lack of long range order and the evidence of self-trapping in-a deep quantum well with a width of about 10 lattice spacings, consistent with Fig. 9. Also note that the shoulders rise above 0.5, suggesting greater than average density on either side of the well due to the addition of atoms excluded from the well. This can also be seen in Fig. 6.

V. COMPARISON WITH MEAN FIELD THEORY

We also compared our results from Monte Carlo calculation with the results from the Mean Field Theory (MFT), which was generally used in previous work.[7, 12]

In MFT, we consider that the state vector $\vec{\Psi}$ acts as an external field for the atoms $\vec{n}$. We minimize the free energy under the constraint $\langle \vec{\Psi} \mid \vec{\Psi} \rangle = 1$ to obtain a difference equation for the components of the wave function:

$$\Psi_{j+1} = -\Psi_{j-1} + \left(\left(\frac{\varepsilon}{1 + \exp[\beta(\varepsilon \Psi_j^2 - \mu)]} \right) - E' \right) \Psi_j \tag{74}$$

Equation (89) was solved iteratively for the ground state by a shooting method which required a reflection symmetric, positive, monotonically decreasing solution which vanished at infinity.

MFT is a rough approximation, but at very low temperature we expect that the qp tends to occupy a single quantum state and, therefore, that MFT should yield results close to the numerically accurate Monte

Table 1. Average Kinetic Energy over a Range of Temperatures for a Particle in Lattice Gas. Monte Carlo Compared with MFT

β	Monte Carlo	MFT
0.1	1.796401	0.16129
0.2	1.645506	0.92217
0.3	1.530350	1.1105
0.4	1.429636	1.1632
0.5	1.339505	1.1731
0.6	1.238408	1.1657
0.7	1.155905	1.1495
0.8	1.082056	1.1268
0.9	0.998696	1.0968
1.0	0.928160	1.0540
2.0	0.522176	0.4311
3.0	0.367641	0.4249
4.0	0.291020	0.4179
5.0	0.246333	0.2213
6.0	0.211787	0.2170
7.0	0.183894	0.2158
8.0	0.166528	0.2150
9.0	0.152720	0.2142
10.0	0.138285	0.2130
100.0	0.012466	0.03541

Table 2. Average Potential Energy over a Range of Temperatures for a Particle in Lattice Gas. Monte Carlo Compared with MFT

β	Monte Carlo	MFT
0.1	2.714219	4.40371
0.2	1.217209	2.05930
0.3	0.537491	1.05604
0.4	0.254720	0.65375
0.5	0.148904	0.49638
0.6	0.111876	0.43731
0.7	0.100211	0.41855
0.8	0.093194	0.41673
0.9	0.087584	0.42324
1.0	0.086344	0.43819
2.0	0.057635	0.09877
3.0	0.039945	0.07358
4.0	0.031121	0.07411
5.0	0.025610	0.04573
6.0	0.022528	0.02996
7.0	0.019232	0.02573
8.0	0.016032	0.02454
9.0	0.014008	0.02470
10.0	0.013047	0.02446
100.0	0.0016421	0.0015555

Carlo calculations. With the exception of a weak local maximum in the MFT results at an inverse temperature of about 0.5 which we are unable to explain at this time, in general both MFT and PIMC show a steady increase in kinetic energy with temperature. When $\beta = 100$ (low temperature) and $\varepsilon = 10$ (strong interaction), we find from MFT that, in our dimensionless units, the kinetic energy of the qp is $\mathrm{KE} = 0.03541$ and the potential energy $\mathrm{PE} = 0.0016421$. However, Monte Carlo yields $\mathrm{KE} = 0.012466$, $\mathrm{PE} = 0.0015555$ for the same temperature and mean lattice density. See Tables 1 and 2 for a further comparison of Monte Carlo results with MFT.

VI. SUMMARY AND CONCLUSIONS

We started with the tight binding Hamiltonian to study a light quantum particle interacting with a lattice gas of atoms. In the case of the free particle we derived the analytically exact solution of eigen energies and wave functions for the system. We investigated system properties in the canonical ensemble such as the partition function, energy, energy fluctuation and self-correlation of the free qp. Using the path integral formalism,

we established a connection between the quantum trace and the weighted sum of variable step size random walks on the lattice. The isomorphism was used to establish a method for carrying out Monte Carlo calculations of the thermal average of physical observables. The Monte Carlo simulation results for the free particle were very well corroborated by the analytical results. Although in the presence of interaction with atoms analytical results cannot be obtained, it's clear that the Monte Carlo method can be trusted.

In the presence of interaction of the qp with the lattice atoms we investigated the kinetic and potential energy and the qp-atom correlation function in the grand canonical ensemble. We considered three distinct cases, two of them characterized by a quenched lattice gas in which the atoms were distributed either periodically or completely disordered, and the third in which the qp-atom system was fully annealed. Localization is demonstrated through the potential energy and qp-atom correlation. Studies of the quenched disordered system exhibited the effects of weak (Anderson) localization whereas the fully annealed system exhibited strong localization due to self-trapping.

We also compared our results with mean field theory, which has been widely used as an approximation in the study of thermalized electrons, positrons and positronium.[1, 2, 7, 12] We found that at low temperature MFT is a good predictor for potential energy but just gives order of magnitude agreement for kinetic energy. As far as we know, this is the first direct comparison of MFT with numerically accurate Monte Carlo predictions.

It is clear that this simple model reproduces the central features of the experimentally observed behavior of light particles in fluids. Moreover, computations can' be carried out much more efficiently than in spatially continuous systems, so it is possible to investigate a much greater range of system parameters with numerical accuracy. In future work we plan to study the case where there are additional interactions between the lattice atoms. We are also going to generalize the lattice from one to two dimensions. In the one dimensional model, no phase transition can occur. In two dimensions, the isomorphism between the interacting lattice gas and the Ising model[25] guarantees a phase transition, and a critical point, in the former. In continuous systems the critical point seems to play an important role in self trapping.[1, 4–7, 12] As mentioned above, in earlier work we have shown that the influence of fluctuations in the critical region is on the same order as the mean field.[18] However, the critical region is very difficult to investigate theoretically and numerically in continuous systems because the convergence is slow. We plan to thoroughly investigate the behavior of a qp in a 2-dimensional interacting lattice gas in the critical region.

ACKNOWLEDGMENTS

The authors appreciate the support of the Research Foundation of and the Department of Information Services of Texas Christian University. One of us also benefitted from conversations with Jaan Oitmaa.

REFERENCES

1. J. Hernandez, *Rev. Mod. Phys.* **63**:675 (1991); D. Chandler and K. Leung, *Annu. Rev. Phys. Chem.* **45**:557 (1994); G. N. Chuev, *Izv. Akad. Nauk., Ser. Fiz.* **61**:1770 (1997).
2. For a review of both experimental and theoretical physics of positron annihilation in fluids see I. T. Iakubov and A. G. Khrapak, *Prog. Phys.* **45**:697 (1982).
3. J. D. McNutt and S. C. Scharma, *J. Chem. Phys.* **68**:130 (1978). S. C. Sharma, R. H. Arganbright, and M. H. Ward, *J. Phys. B* **20**:867 (1987); S. C. Sharma and E. H. Juenguman, *Phys. Lett. A* **144**:47 (1986).
4. P. Hautojarvi, K. Rytsola, P. Tuovinen, and P. Jauho, *Phys. Lett. A* **57**:175 (1976).
5. N. Gee and G. R. Freeman, *Can. J. Chem.* **64**:1810 (1986).
6. A. F. Borghesani and M. Santini, *Linking the Gaseous and Condensed Phases of Matter: The Behavior of Slow Electrons*, L. G. Christophorou, E. Illenberger, and W. Schmidt, eds. (Plenum, New York, 1994, Vol. 326); *Phys. Rev. A* **45**:8803 (1992).
7. M. J. Stott and E. Zaremba, *Phys. Rev. Lett.* **38**:1493 (1977).
8. B. Plenkiewicz, Y. Frongillo, and J. P. Jay-Gerin, *Phys. Rev. E* **47**:419 (1993).
9. M. H. Cohen and J. Lekner, *Phys. Rev.* **158**:305 (1967).
10. G. N. Chuev, *J. Exp. Th. Phys.* **88**:807 (1999).
11. K. Ishi, *Prog. Theor. Phys. Supp.* **53**:77 (1973).
12. M. Tuomisaari, K. Rytsola, and P. Hautojarvi, *J. Phys. B* **21**:3917 (1988); T. J. Murphy and C. M. Surko, *J. Phys. B* **23**:L727 (1990).
13. B. N. Miller and T. Reese, *Phys. Rev. A* **39**:4735 (1989).
14. R. P. Feynman, *Statistical Mechanics* (Benjamin, Reading, MA, 1972).
15. G. A. Worrell and B. N. Miller, *Phys. Rev. A* **46**:3380 (1992).
16. T. L. Reese and B. N. Miller, *Phys. Rev. E* **47**:2581 (1993).
17. B. J. Berne and D. Thirumali, *Ann. Rev. Phys.* **37**:401 (1986); J. S. Bader, B. J. Nerne, and P. Hanggi, *J. Chem. Phys.* **106**:2372 (1997); J. Cao and B. J. Berne, *J. Chem. Phys.* **99**:2902 (1993).
18. B. N. Miller, T. L. Reese, and G. A. Worrell, *Phys. Rev. E* **47**:4083 (1993).
19. A. L. Nichols III, D. Chandler, Y. Singh, and D. M. Richardson, *J. Chem. Phys.* **81**:5109 (1984).
20. J. Chen and B. N. Miller, *Phys. Rev. E* **48**:3667 (1993).
21. J. Chen and B. N. Miller, *J. Chem. Phys.* **100**:3013 (1994).
22. J. Chen and B. N. Miller, *Phys. Rev. B* **49**:615 (1994).
23. I. Chang, K. Ikeyawa, and M. Kohmoto, *Phys. Rev. B* **55**:12971 (1997); N. W. Ashcroft and D. Mermin, *Solid State Physics* (Holt, Rinehart, and Winston, 1976).
24. M. H. Kalos and P. A. Whitlock, *Monte Carlo Methods Volume I: Basics* (John Wiley, New York, 1986).
25. R. K. Pathria, *Statistical Mechanics*, 2nd ed. (Butterworth–Heinemann, 1996).